Particle Accelerators
1976, Vol. 7, pp. 245–253

DECELERATION OF ELECTRON RINGS BY IONS

U. SCHUMACHER, I. HOFMANN, and P. MERKEL

Max-Planck-Institut für Plasmaphysik, D-8046 Garching bei München, BRD

and

M. REISER

University of Maryland, College Park, Maryland 20742, U.S.A.

(*Received June 26, 1976; in final form August 13, 1976*)

The deceleration of intense relativistic electron rings by ions that are created by impact ionization in the electron rings is calculated analytically and numerically. It turns out that the stopping of rings with initial axial velocities of about $\beta_o = 0.1$ is possible under conditions, that easily can be realized experimentally in the Maryland ERA. The stopping length of the electron rings, however, depends sensitively on the initial axial ring velocities β_o (as β_o^3). If the method of ring deceleration by ions is used, the reproducibility of the initial ring parameters (especially that of β_o) should be very good to get reliable electron ring loading and acceleration.

I INTRODUCTION

In one of the devices for electron ring acceleration (ERA), the Maryland scheme,[1] an intense relativistic electron ring is formed by the passage of a hollow electron beam through a cusped magnetic field, which transforms axial into rotational velocity. The axial velocity of the electrons after the passage of the cusped field, however, is still in the range of $dz_e/dt = \beta_o c = 0.1c$, where c is the speed of light. To further slow down the electrons to axial velocities where the trapping of ions in the electron ring is possible, different methods may be applied, such as the trapping of the ring in a fast pulsed mirror magnetic field,[3,4] the stopping by resistive wires[5] or cylinders,[6,7] or the deceleration by ions, that are produced by impact ionization in the electron ring and that are partly accelerated before escaping from the ring potential well.

In this report the method of ring deceleration by ions is treated analytically and numerically, and computational results are presented for several examples with parameter values close to those of the Maryland ERA device.

II ANALYTICAL CONSIDERATIONS

In an electron ring of N_e electrons the ions are created at a rate of

$$dN_i/dt = \alpha N_e, \tag{1}$$

where α is given by the pressure p of the background gas. Normally α is a function of time and of space. In order to estimate the stopping length z_{tr}, the stopping time t_{tr} and the required ion number N_i (normalized to N_e) for the deceleration and the stopping of the electron ring by ions, we simplify our analytical calculations by assuming α to be independent of space, time and energy. (For spatial variation of α see Section IV.) The energy dependence of α can be ignored, since the ionization cross section of electrons with energies above 1 MeV is nearly independent of the electron energy and, moreover, the total electron energy changes only slightly during the process under consideration.

If the electron ring is moving with an axial velocity v_e, which is so high that the ions cannot be trapped in the ring, the ion number $\tilde{N}_i$ in the

ring is approximately given by

$$\tilde{N}_i/N_e = \alpha \frac{b}{v_e},$$

where b is the minor half axis of the electron ring.

The ions created by impact ionization in the potential well of the electron ring gain a potential energy that depends on the location of their creation in the ring as well as on the ring boundary conditions. In the special case of an electron ring with a circular beam cross section and uniform electron density, that is near to an image cylinder, the average potential depth ΔU is roughly given by half the value of the full potential difference.

From the conservation of energy and momentum of the electrons and ions follows that the ions are accelerated to an average velocity v_i, which is given by

$$v_i = \frac{v_e}{1 + \alpha \frac{b}{v_c} \cdot \frac{M_i}{m_e \gamma} \cdot \left(1 - \sqrt{1 - \frac{e\Delta U}{M_i v_e^2/2} \cdot \left(1 + \alpha \frac{b}{v_e} \cdot \frac{M_i}{m_e \gamma}\right)}\right)}, \quad (2)$$

where M_i is the ion mass and $m_e\gamma$ the (relativistic) electron mass. The square root in Eq. (2) vanishes, if the trapping velocity v_{tr} of the electron ring is reached.

Each ion that is created with a single charge near the electron ring center takes the energy

$$W_i = \frac{M_i}{2} v_i^2 + e\Delta U$$

from the electron ring. The rate of energy loss by the electron ring is then given by

$$\frac{dW}{dt} = N_e \gamma \frac{m_e}{2} \frac{dv_e^2}{dt} = -\frac{dN_i}{dt}\left\{e\Delta U + \frac{M_i}{2} v_i^2\right\}. \quad (3)$$

The energy loss due to the secondary electrons created in each collision is neglected because of the nearly isotropic emission under our conditions.

As initially

$$v_e^2 \gg \frac{2e\Delta U}{M_i}\left(1 + \alpha \frac{b}{v_c} \frac{M_i}{m_e \gamma}\right) \quad (3a)$$

in all cases under consideration, $M_i v_i^2/2$ can be neglected compared to $e\Delta U$ in Eq. (3).

Equation (3) results in estimates for the length, the time, and the ion number needed for the stopping of electron rings with an intial β_o and we find with Eq. (1)

$$\gamma \frac{m_e}{2} \frac{dv_e^2}{dt} = \gamma \frac{m_e}{2} v_e \frac{dv_e^2}{dz} = -\alpha e \Delta U,$$

and the stopping length z_{tr} is about

$$z_{tr} \simeq -\int_{v_{eo}}^{v_{tr}} \frac{\gamma m_e}{2\alpha e \Delta U} v_e dv_e^2 \simeq \frac{\gamma m_e}{3\alpha e \Delta U} v_{eo}^3$$

$$= \frac{\gamma m_e}{3\alpha e \Delta U} c^3 \beta_o^3 \quad (4)$$

The stopping time t_{tr} is given by

$$t_{tr} \simeq \frac{\gamma m_e}{2\alpha e \Delta U} \int_{v_{eo}}^{v_{tr}} dv_e^2 \simeq \frac{\gamma m_e}{2\alpha e \Delta U} v_{eo}^2 = \frac{\gamma m_e}{2\alpha e \Delta U} c^2 \beta_o^2, \quad (5)$$

and the ion number N_i (normalized to N_e), needed for stopping is approximately

$$\frac{N_i}{N_e} \simeq -\frac{\gamma m_e}{2e\Delta U} \int_{v_{eo}}^{v_{tr}} dv_e^2 \simeq \frac{\gamma m_e}{2e\Delta U} v_{eo}^2 = \frac{\gamma m_e}{2e\Delta U} c^2 \beta_o^2 \quad (6)$$

with the relations

$$z_{tr} \simeq \frac{2}{3} \frac{c\beta_o}{\alpha} \cdot \frac{N_i}{N_e} \quad (7)$$

and

$$t_{tr} \simeq \frac{1}{\alpha} \frac{N_i}{N_e} = \frac{3}{2c\beta_o} \cdot z_{tr}. \quad (8)$$

At the end of the stopping process the inequality (3a) is violated. The electron ring now does not only lose energy due to lifting the ions to higher potential but also due to accelerating the ions collectively (after their capture) to the final electron ring axial speed. The effect on the calculated quantities in Eqs. (4) to (8), however, turns out to be negligible for the initial axial velocities $c\beta_o$ under consideration.

To get a feeling whether the stopping of electron rings with initial axial velocities in the order of $c\beta_o = 0.1 \cdot c$ can be realized experimentally, we choose the following example:

$\gamma = 5, e\Delta U = 0.1$ MeV, $\beta_o = 0.1$ and $z_{tr} = 30$ cm

and we obtain from Eqs. (6) to (8)

$$\frac{N_i}{N_e} = 0.127; t_{tr} \simeq 15 \text{ ns and } \alpha \simeq 8.46 \cdot 10^6 \text{ s}^{-1}.$$

The ionization coefficient α is roughly given[2] by $\alpha(\text{s}^{-1}) \simeq 1.064 \cdot 10^8 \cdot Z_M \cdot p(\text{Torr})$, where Z_M is the

number of electrons per molecule. In forming this relation we used an ionization cross section of $\sigma = 10^{-19}$ cm^2 (for electrons of more than 1 MeV kinetic energy on H or He atoms). To obtain the desired ion number one needs in the case of hydrogen ($Z_M = 2$) a pressure of $p \simeq 4 \times 10^{-2}$ Torr.

The example chosen demonstrates that the stopping of electron rings by ions is possible under conditions that can be realized in the Maryland ERA experiment. The required gas pressure, however, seems to be relatively high compared to the vacuum requirements in the acceleration section.

Furthermore the cubic dependence of the stopping length z_{tr} on the initial ring axial speed β_o (Eq. 4) imposes stringent limitations on the reproducibility of the initial ring parameters.

In the following the stopping of the electron ring by ions is treated numerically.

III NUMERICAL CALCULATIONS

For the numerical treatment of the problem of deceleration of electron rings by ions the equations of motion of the electron ring and several ion subrings are solved with a computer program that was developed for similar problems.[8] It is assumed, that ions are created by impact ionization in the electron rings, that they are accelerated by the electric field of the electron ring and—if the electron ring speed is too high—escape from the ring. The electron ring as well as the ion subrings are regarded to be rigid. This assumption of unchanged electron ring shape appears to be reasonable, if the axial focussing of the electron ring is done by an image field cylinder ("squirrel cage") independently of the ions. In fact, it was found theoretically[9] and experimentally[10,11] that image focussing of the electron ring results in considerably higher collective ion acceleration (high holding power) than focussing by ions.

The electron density distribution n_e is assumed to be a Gaussian one, i.e.,

$$n_e(r) = n_e(o)\exp(-r^2/r_o^2),$$

where r is the distance from the center of the ring minor cross section.

Dividing the ions into K subrings and neglecting the toroidicity (i.e., solving the straight beam problem) the equations for the motion in axial direction are

$$m_e\gamma\ddot{z}_e = c\beta_0 B_r(z)e - \sum_{j=1}^{K} \frac{e^2 N_{i,j}\cdot z_j}{4\pi^2 R\varepsilon_o}\cdot\frac{1}{z_e - z_{i,j}} \left[1 - \exp\left\{-\left(\frac{z_e - z_{i,j}}{r_o}\right)^2\right\}\right] \cdot\left\{1 - \frac{1}{1 + [d/(z_e - z_{i,j})]^2}\right\} \tag{9a}$$

$$M_i\ddot{z}_{i,j} = \frac{e^2 N_e\cdot Z_j}{4\pi^2 R\varepsilon_o}\cdot\frac{1}{z_e - z_{i,j}} \cdot\left[1 - \exp\left\{-\left(\frac{z_e - z_{i,j}}{r_o}\right)^2\right\}\right] \cdot\left\{1 - \frac{1}{1 + [d/(z_e - z_{i,j})]^2}\right\} \tag{9b}$$

$$j = 1, K$$

z_e and $z_{i,j}$ are the axial locations of the electron ring and the j-th ion subring, respectively. N_e is the total number of electrons and $N_{i,j}$ the number of ions in the j-th ion subring. Z_j is the charge per ion in the j-th ring and d is the distance from the electron ring to an image field cylinder ("squirrel cage"). β_0 is the azimuthal electron velocity normalized to the speed of light c.

The image field cylinder turns out to be necessary for additional axial focussing of the ring, so that its influence is included approximately in the above equations through an additional term in the force equations involving the distance between real charge and image charge distributions. These image fields reduce the coupling of the ion rings to the electron ring, especially at long distances between the ions and the electron ring center.

The coupling of the ion subrings to each other is neglected, as well as that of the secondary electrons, that are created at every ionization process.

In the following some examples of the numerical calculations are given for electron rings of $r_o = 0.5$ cm, $R = 6$ cm major radius and $d = 0.7$ cm distance to the image cylinder and maximum electric field strength of $E_{max} = 0.44\cdot eN_e/4\pi^2\varepsilon_o Rr_o = 4.4$ MV/m (the factor 0.44 takes the Gaussian distribution and the image fields into account). The potential depth is $\Delta U = 0.04$ MV. In Figure 1 protons ($M_i = m_p$) are created each 2 ns in the electron ring, that initially has an axial speed of $c\beta_o = 0.02\cdot c$. The ratio of total number of ions produced N_i to that of the electrons is $N_i/N_e = 0.02$.

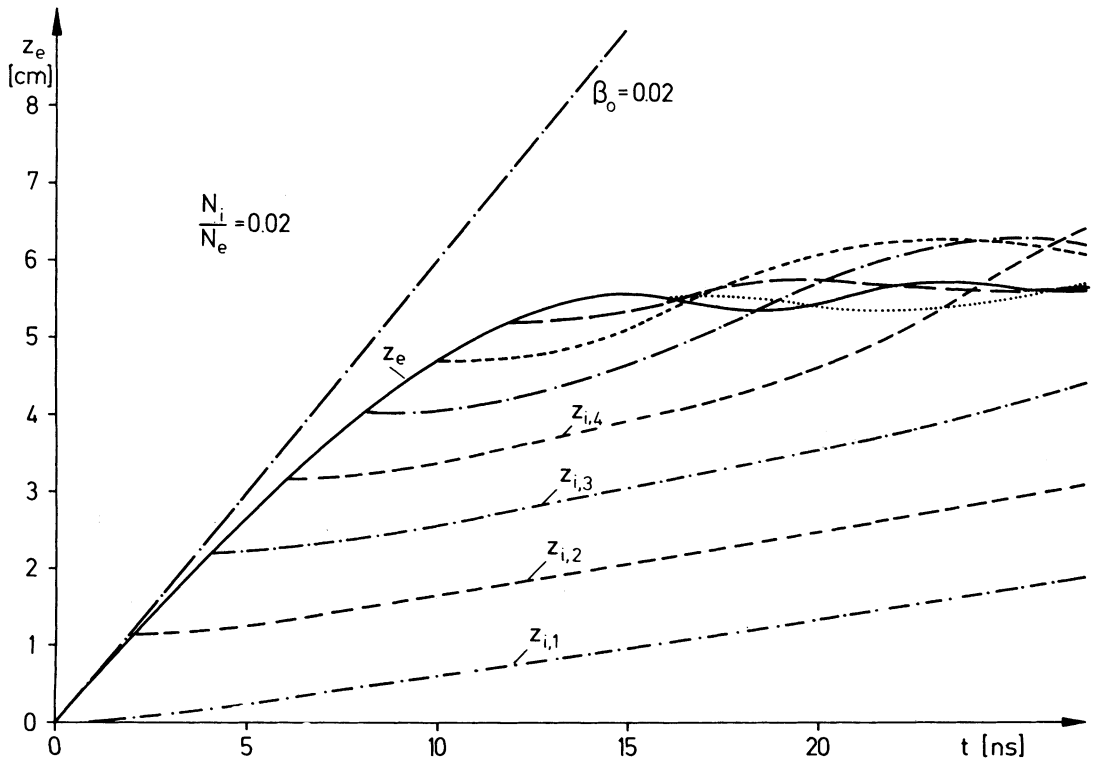

FIGURE 1 The axial positions of the electron ring and of protons versus time for $\beta_o = 0.02$.

The axial positions of the electron ring z_e and those of the ions $z_{i,j}$ (dotted lines) are plotted versus the time. As can be seen from these plots the ions gain energy from the electrons; as a result, the electron ring quickly decelerates and actually stops at a distance of about 5 cm. But the ions, that had escaped earlier, catch up and interact with the electron ring. This leads to axial oscillations so that only a small fraction of the ions remains trapped in the electron ring. In this case the ions are assumed to be produced every 2 ns at the center of the electron ring, where the potential minimum is located. The creation of ions all over the electron ring corresponding to the electron density gives similar results.

The stopping length of the electron ring depends on the gas pressure used (or the total number of ions produced) and on the initial axial ring velocity $\beta_o c$. Figure 2 shows (for an ionization interval of 10 ns) the deceleration of the electron ring for different applied gas pressures expressed in terms of the total number of ions produced relative to the electron number. Under the condition of electron rings with initial $\beta_o = 0.1$, total ionization fractions of $N_i/N_e = 0.3$ to 0.4 produced in 10 ns are necessary for ring stopping at a length of about 15 to 20 cm.

The dependence of the deceleration effect on the initial axial velocity β_o of the electron ring is illustrated in Figure 3 for the same ionization interval of 10 ns. The stopping length depends on the initial β_o. A ring with $\beta_o = 0.08$ is stopped at $z = 8$ cm, that with $\beta_o = 0.1$ at about $z = 16$ cm, and for $\beta_o = 0.12$ the ionization interval is too short or the total number of ions produced is too small, respectively, to obtain complete stopping of the ring.

In the case of $\beta_o = 0.11$ the energy balance can easily be checked at $t \simeq 11$ ns, where the electron ring axial velocity has come to zero and its initial kinetic energy

$$E_{eo} = \tfrac{1}{2} m_e \gamma \beta_o^2 c^2$$

has been transferred to the kinetic and potential energy of the ions:

$$E_{\text{kin}} = 3.77 \cdot 10^{-9}\ \text{gcm}^2/\text{s}^2$$

and

$$E_{\text{pot}} = 2.18 \cdot 10^{-8}\ \text{gcm}^2/\text{s}^2.$$

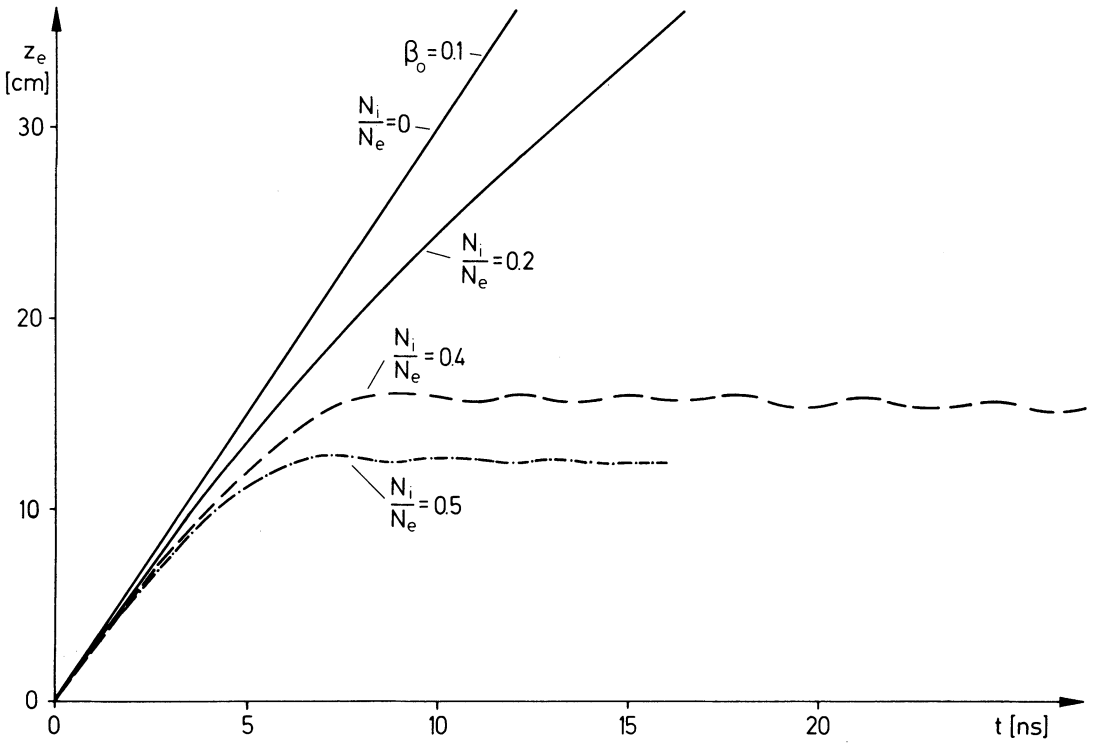

FIGURE 2 The electron ring motion for different total ion numbers.

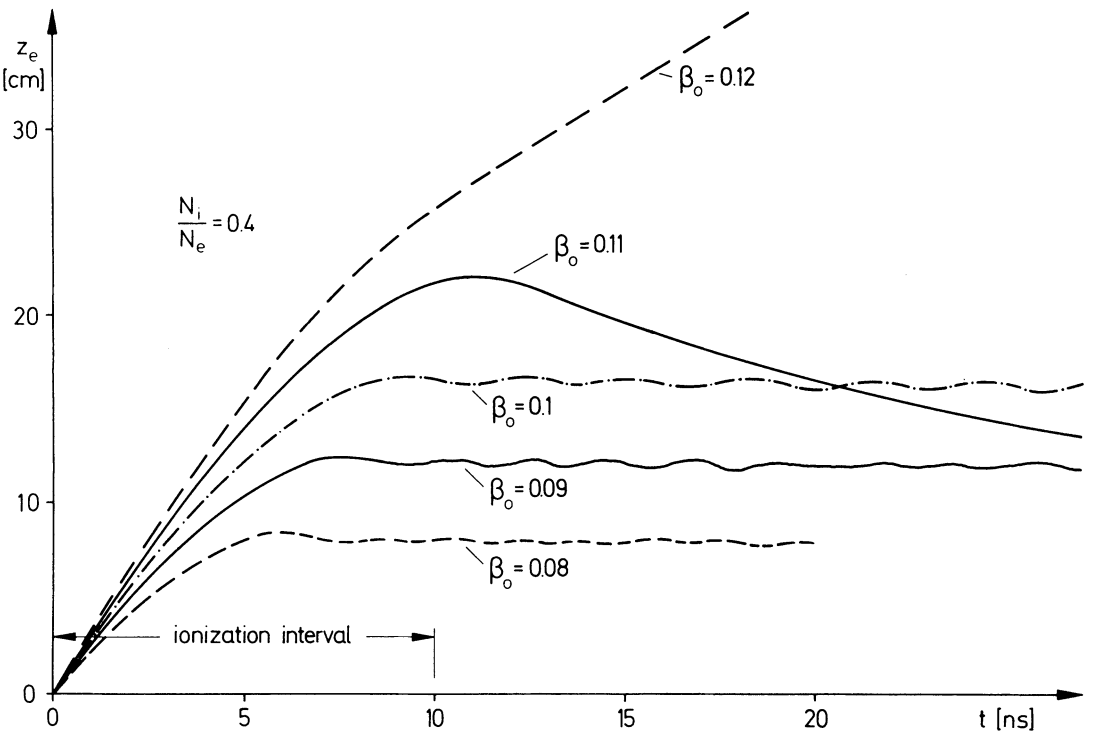

FIGURE 3 The electron ring motion for different initial axial velocities $\beta_o \cdot c$.

The corresponding β, calculated from

$$\beta^2 = \frac{2(E_{kin} + E_{pot})}{m_e \gamma c^2}$$

is $\beta = 0.112$, which is in relative good agreement with the initial $\beta_o = 0.11$ of the electron ring.

The decrease of the electron ring velocity dz_e/dt for the same conditions as in Figure 3 is plotted in Figure 4 versus the time; as expected, the strongest decrease is at smaller velocities. This is even more obvious in the plot of the electron ring deceleration $(-d^2z_e/dt^2)$ in Figure 5 versus the axial distance. These curves show a Bragg-peak and demonstrate the sensitive dependence of the stopping length z_{tr} (where the ions are trapped) from the initial ring velocity β_o.

The stopping length z_{tr} is found to be proportional to the third power of β_o

$$z_{tr} \sim \beta_o^3$$

in agreement with the analytic result in Eq. (4). Integration of the deceleration over z from zero to the stopping point reproduces fairly well the analytically expected value given by

$$-\int_0^{z_{tr}} \frac{d^2 z_c}{dt^2} dz = \frac{1}{2} c^2 \beta_o^2$$

Figure 6 summarizes the dependence of the stopping length z_{tr} and the ion loading $\tilde{N}_i/N_e$ of the rings (at $t = 50$ ns) under the conditions of Figure 3. Both the stopping length and the ion loading fraction depend very sensitively on the initial electron velocity β_o.

While for the calculations mentioned so far the radial magnetic field component B_r in Eq. (9a) has been chosen to vanish, Figure 7 gives an example of the application of $B_r \simeq 4$ G for axial positions $z \gtrsim 15$ cm. Again, as the figure indicates, the initial β_o has to be chosen very carefully to get the desired result of stopping, ion loading and acceleration of the electron rings.

Because of the sensitive dependence of the stopping length and ion loading fraction on the initial electron ring velocity β_o the practical application of this method of ring stopping demands a very good reproducibility of the electron ring initial properties.

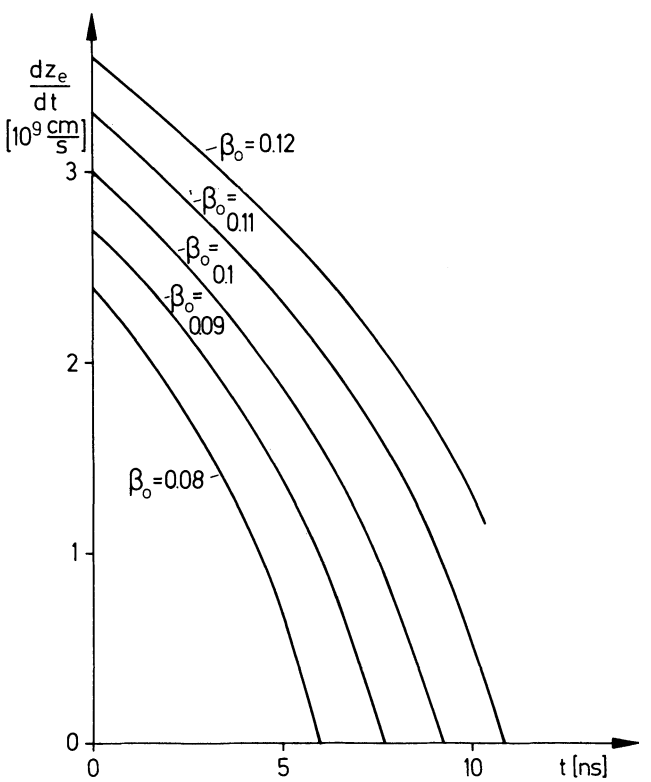

FIGURE 4 The electron velocity for different β_o.

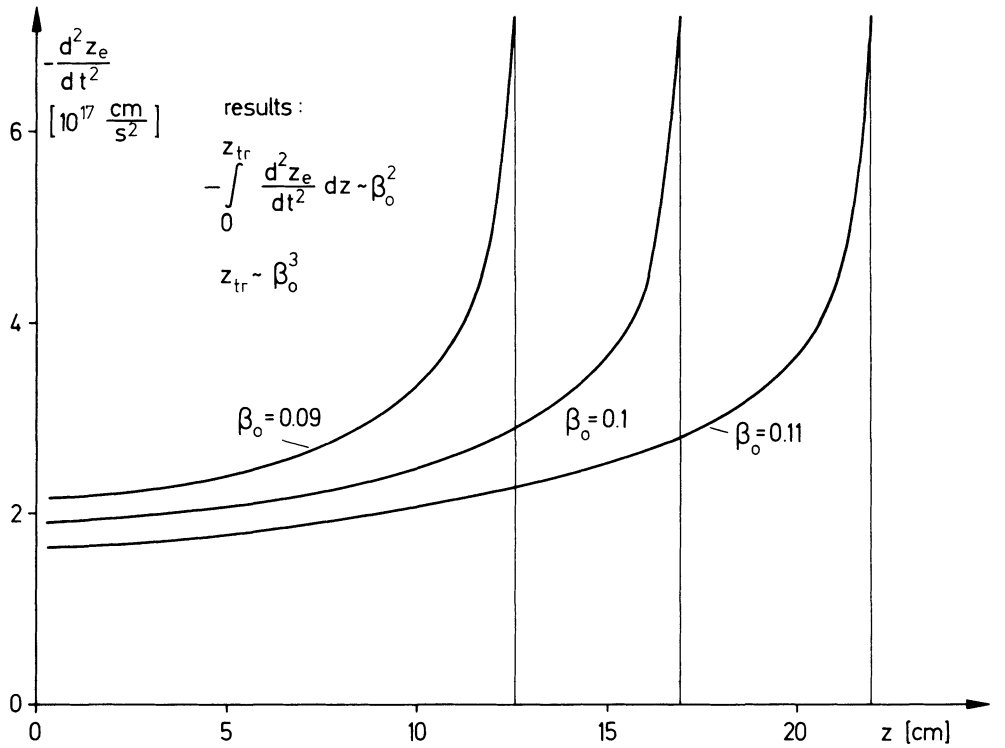

FIGURE 5 The electron ring deceleration for different β_o.

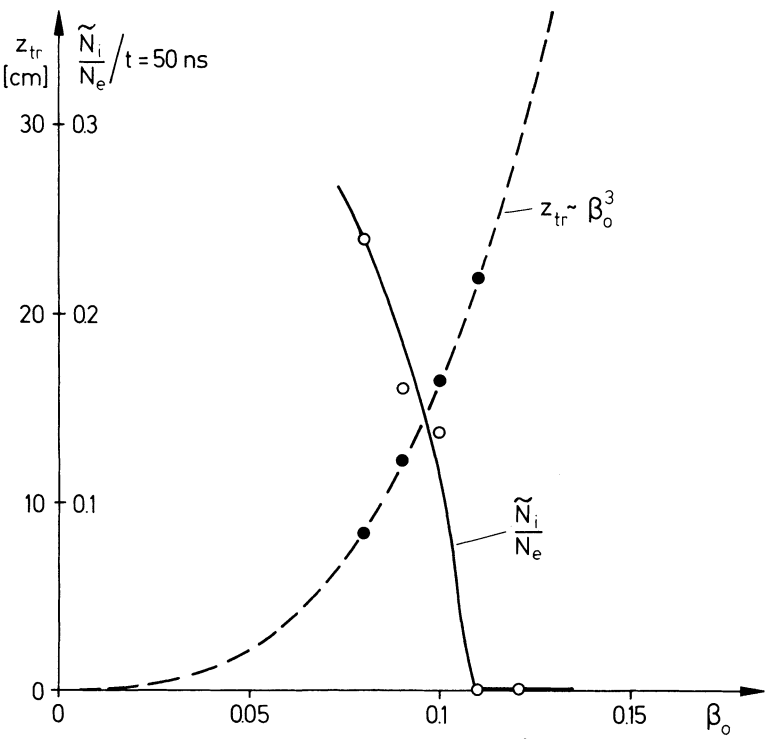

FIGURE 6 The dependence of z_{tr} and $\tilde{N}_i/N_e$ on β_o.

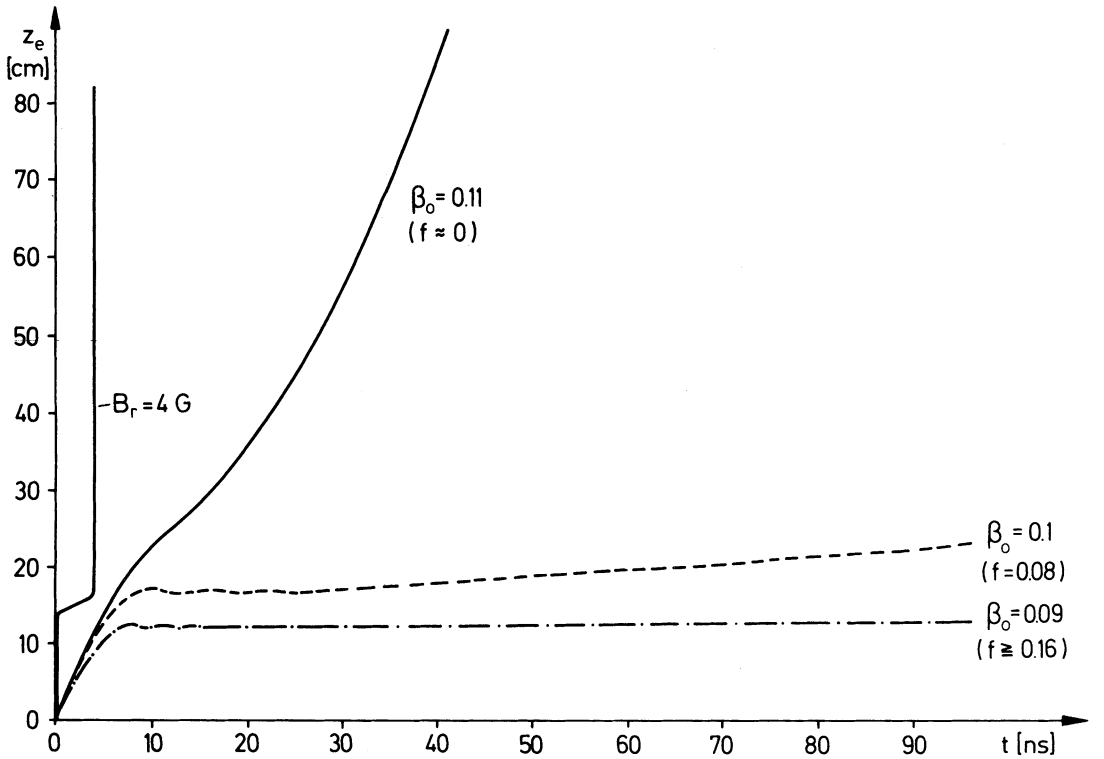

FIGURE 7 The ring motion for different β_0 with a superimposed B_r-field.

IV APPLICATION

In the calculations the pressure always was assumed to be constant. In the actual experiment at Maryland, however, the pressure varies with distance [$p = p(z)$], as it is produced by opening of a puff valve. A typical curve (according to the measurements of Misra[12]) is plotted in Figure 8. Both peak pressure p_o as well as the "width" Δz of this p versus z curve can be varied experimentally by increasing the amount of gas in the "puff" or by injecting the electron ring at a different time after opening the puff valve. At later times the $p(z)$ curve gets flatter and broader, for instance.

The spatial variation of the pressure p is taken into account by the relation

$$dN_i = N_e \alpha(z) dz / v_e .$$

The pressure pulse shape should have a certain axial distribution for a successful experiment. Since the electron ring axial velocity decreases due to the ion stopping, there is a speed, where some of the ions may catch up with the ring. before it enters the acceleration region. To avoid overloading of the ring, it appears better to work with a

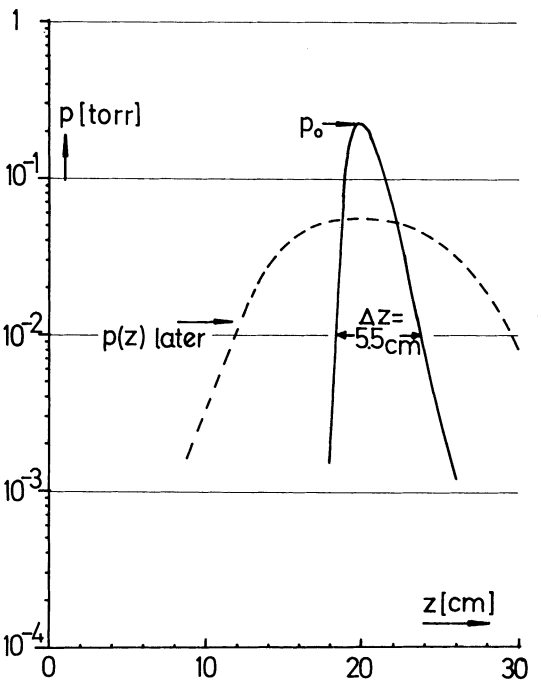

FIGURE 8 The axial pressure distribution as obtained with a puff valve (from Ref. 12, Figure 33).

broad pressure pulse shape rather than the sharp curve shown in the figure.

Let z_{tr} be the position downstream from the cusp where the electron ring is slowed down to the trapping velocity v_{tr}. The number of ions that are loaded into the ring is then determined by the integral

$$\int_{z_{tr}}^{z_{acc}} \frac{\alpha(z)}{v_e(z)}\, dz,$$

where z_{acc} is the beginning of the expansion–acceleration region. An important problem for the experiment is how to control this integral to avoid overloading, which results in very low final ion energy, or underloading, so that the ring acceleration is too high and all ions are lost.

The application of this method of electron ring deceleration and ion loading requires good reproducibility of the operating parameters, especially the initial axial velocity $\beta_o c$ of the electron ring.

ACKNOWLEDGEMENTS

This work was performed under the terms of the agreement on association between the Max-Planck-Institut für Plasmaphysik and EURATOM. The authors are grateful to E. Springmann who carried out the numerical calculations.

REFERENCES

1. M. Reiser, *IEEE Trans. Nucl. Sci.*, **NS-18**, 460 (1971).
2. M. Reiser, *IEEE Trans. Nucl. Sci.*, **NS-19**, 280 (1972).
3. M. Reiser, *IEEE Trans. Nucl. Sci.*, **NS-20**, 310 (1973).
4. W. W. Destler, A. Greenwald, D. W. Hudgings, H. Kim, P. K. Misra, M. P. Reiser, M. J. Rhee, and G. T. Zorn, *Proc. IXth Int. Conf. on High Energy Accelerators*, Stanford, Cal., USA, May 2–7, 1974, p. 230.
5. J. G. Kalnins, H. Kim, and J. G. Linhart, *IEEE Trans. Nucl. Sci.*, **NS-20**, 324 (1973).
6. P. Merkel, MPI für Plasmaphysik, Garching, Report 0/24, Oct. 74, and *Part. Accelerators*, **7**, 69 (1976).
7. W. Herrmann, MPI für Plasmaphysik, Garching, Report 0/25, Nov. 74, and *Part. Accelerators*, **7**, 19 (1975).
8. U. Schumacher, MPI für Plasmaphysik, Garching, Report in preparation.
9. I. Hofmann, *Proc. IXth Int. Conf. on High Energy Accelerators*, Stanford, Cal., USA, May 2–7, 1974, p. 245.
10. C. Andelfinger, W. Dommaschk, I. Hofmann, P. Merkel, U. Schumacher, and M. Ulrich, *Proc. IXth Int. Conf. on High Energy Accelerators*, Stanford, Cal., USA, May 2–7, 1974, p. 218.
11. U. Schumacher, C. Andelfinger, and M. Ulrich, *IEEE Trans. Nucl. Sci.*, **NS-22**, 989 (1975).
12. P. K. Misra, Studies of Intense Relativistic, Hollow Electron Beam Dynamics in the Cusped Magnetic Field of the Maryland Electron Ring Accelerator, Ph.D. Thesis, Elect. Eng. Dept., University of Maryland, College Park, Maryland, USA, 1975.